13

Secondary eyewall formation in tropical cyclones

Chun-Chieh Wu, Yi-Hsuan Huang, and Zhemin Tan

13.1 Introduction

Secondary eyewall formation (SEF), and the subsequent eyewall replacement cycle, are often observed in intense tropical cyclones (TCs), and its association with short-term changes in TC intensity and structure has been widely documented from aircraft observations and satellite imagery (Willoughby *et al*., 1982, Black and Willoughby, 1992, Willoughby and Black, 1996, Houze *et al*., 2006, 2007, Hawkins and Helveston, 2008, Kossin and Sitkowski, 2009, Kuo *et al*., 2009, Didlake and Houze, 2011, Sitkowski *et al*., 2011, Bell *et al*., 2012, Hence and Houze, 2012). A double-eyewall TC contains two concentric quasi-circular deep convective rings (inner and outer TC eyewalls) with a nearly cloud-free region (moat) between them. In most such cases, the outer eyewall is established later, with characteristics similar to the inner eyewall. A localized maximum swirling wind is often present in the outer eyewall, with its scope confined to the lower troposphere. Taking the example of a model simulation of Typhoon Sinlaku (2008), constructed by Wu *et al*. (2012), Fig. 13.1 demonstrates such flow characteristics in a concentric eyewall TC. For cases undergoing an eyewall replacement cycle, during which a TC usually weakens and enlarges, the inner eyewall gradually dissipates, while the outer eyewall later becomes the new primary eyewall. More recently, it has been shown that SEF is preceded by a broadening tangential wind field with small radial gradients in the storm's outer-core region, serving as a precursory flow characteristic for SEF (Wu *et al*., 2012, Huang *et al*., 2012; hereafter WH12). Considering such temporary, but pronounced, changes in storm intensity and structure, and the lack of skill in predicting concentric-eyewall events, SEF remains an important research issue and forecast priority for the understanding of TC intensity/structure evolution.

This review provides an updated summary and discussion of the literature concerned with our current understanding of the favorable conditions for, and potential mechanisms of, SEF. Because of limited or discontinuous spatial/temporal coverage of observations, studies of SEF mechanisms have mostly been based on numerical simulations. The remainder of this article is organized as follows. Section 13.2 describes the possible roles of various environmental conditions in SEF. Having considered the environmental factors that are conducive to SEF, Section 13.3 introduces a variety of internal dynamical processes suggested for SEF, such as the axisymmetrization process, energy accumulation through vortex Rossby wave activities, beta-skirt-induced energy cascade, unbalanced responses to boundary layer dynamics, and balanced response to convective heating. Finally, in Section 13.4, the merits and caveats of the various dynamical interpretations are discussed, and the remaining unresolved issues are addressed to provide guidance for future SEF research.

13.2 Environmental conditions

Numerical models of various designs have been used to study the impact of ambient relative humidity on SEF. In the axisymmetric model framework of Nong and Emanuel (2003), high relative humidity is critical to SEF only if the hydrostatic assumption is applied. In contrast, full-physics model simulations have shown that high environmental relative humidity is crucial to the formation of an outer eyewall in a TC (e.g. Hill and Lackmann, 2009, Wang, 2009). Sitkowski *et al*. (2011) presented supporting results for the important role of higher relative humidity in SEF based on observational data. A plausible explanation for this finding is that high ambient humidity provides more moisture and so enhances latent heat release in the vortex's outer-core region. Therefore, the development of convection outside the primary eyewall is enhanced, and, subsequently, the formation/intensification of rainbands and even SEF. Another pathway for environmental influence on SEF, described by Nong and Emanuel (2003), is the

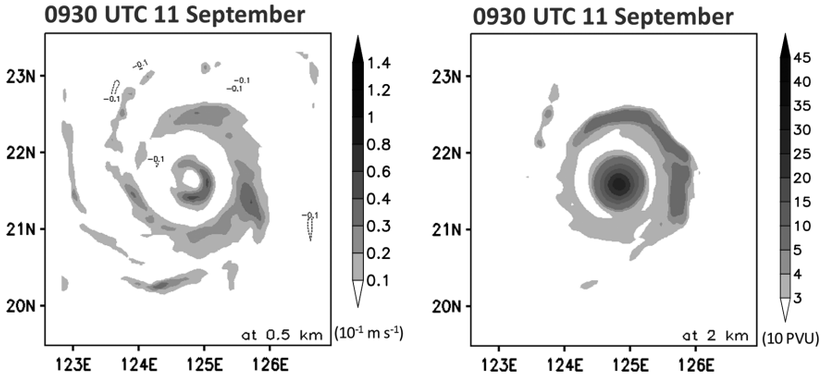

Fig. 13.1. Plan view of vertical velocity (10^{-1} ms^{-1}; left) at 0.5 km and potential vorticity (10 PVU; right) at 2 km at 0930 UTC 11 September when the simulated storm underwent a concentric-eyewall episode.

sustained eddy angular momentum fluxes raised by interactions between a mature TC and its environment. This TC–environment interaction, if sufficiently influential in strength and space, can generate the WISHE (wind-induced surface [air–sea] heat exchange; Yano and Emanuel, 1991) process, which may serve as a promising dynamical means for the establishment of a secondary eyewall outside the primary eyewall.

13.3 Internal mechanisms of SEF

Five internal mechanisms frequently discussed in previous SEF studies are considered in this subsection, namely, vortex Rossby waves, the axisymmetrization process, the beta-skirt axisymmetrization formation hypothesis, unbalanced boundary layer dynamics near the top of the TC boundary layer, and the balanced response to diabatic heating in a region of enhanced inertial stability.

13.3.1 Vortex Rossby waves

Based on radar and satellite images, Macdonald (1968) found that disturbances with similar characteristics to Rossby waves are often associated with TC rainbands, and the term vortex Rossby waves (VRWs) was coined for these eddy activities in TCs. Similarly to Rossby waves in the planetary system, the dispersion relationship for VRWs is closely related to the vorticity gradient. In a dry and barotropic framework, Montgomery and Kallenbach (1997) obtained an analytic solution for the stagnation radius of VRWs that propagate radially outwards from the eyewall. It has since been proposed that the accumulation of energy near that stagnation radius of VRWs contributes to the outer rainbands, and perhaps to SEF (Montgomery and Kallenbach, 1997, Chen and Yau, 2001, Wang, 2002a, b, Chen *et al*., 2003, Corbosiero *et al*., 2006, Martinez *et al*., 2010, 2011, Qiu *et al*., 2010, Abarca and Corbosiero, 2011, Menelaou *et al*., 2012, 2013). While the role of VRWs in TC rainbands has been clarified, the role of VRWs in SEF remains unclear. Recent studies with high-resolution models and more sophisticated physical processes have suggested that VRW activities may not directly contribute to SEF, which is different from results obtained from simple model configurations. Judt and Chen (2010) indicated that the near-zero potential vorticity (PV) gradient, subsidence, and straining effect that are already present prior to SEF are not conducive to the outward propagation of VRWs, suggesting reasonable doubt regarding the essential role of VRWs in SEF. Noting the ambiguous role of the eddy fluxes associated with VRWs in speeding up the tangential wind in the SEF region, Corbosiero *et al*. (2012) inferred that the outward propagation of the convectively coupled VRWs from the inner eyewall may act to redistribute PV and so allow moisture to accumulate at the stagnation radius. This suggests that VRWs make the active convection more prominent, but not to the extent that would directly cause SEF. Sun *et al*. (2013) showed only limited contribution from VRWs to SEF in their simulation of Typhoon Sinlaku.

13.3.2 Axisymmetrization process

The axisymmetrization process, which has been articulated in previous studies on fundamental vortex dynamics (Melander *et al*., 1987, McWilliams, 1990, Dritschel and Waugh, 1992, Fuentes, 2004), has also been used to interpret the formation of a vorticity ring outside the parent vortex in 2D barotropic models. It is suggested that the primary vortex can axisymmetrize weak vorticity patches into a vorticity ring, provided that the primary vortex is strong enough and the two vortices are sufficiently close to each other (Kuo *et al*., 2004, 2008). Kuo *et al.* (2008) indicated that a vorticity skirt (where the radial gradient of vorticity is small) in the vortex's outer-core region

provides an additional flow background that is conducive to the formation of an outer vorticity ring enhanced by the binary-vortex interaction. Nevertheless, recent studies noted that PV patches outside the eyewall, either in the real TC environment or in a simulated TC that considers more realistic physical processes (such as moist convection), can be of comparable magnitude to that in the eyewall region and have dipole structures. Moon *et al*. (2010) demonstrated that the interaction between the TC core vortex and the convection-induced small vorticity dipoles of considerable strength in 2D flows does not lead to the formation of a coherent concentric vorticity ring. Consequently, the axisymmetrization process under a simplified 2D incompressible flow appears insufficient for describing SEF in the real atmosphere. The critical role of the 3D moist process in the maintenance of a vorticity ring has also been demonstrated (e.g. Wu *et al*., 2009).

13.3.3 Beta-skirt axisymmetrization formation hypothesis

Terwey and Montgomery (2008) presented a new moist-based beta-skirt axisymmetrization (BSA) formation hypothesis for SEF. This hypothesis requires a region with a sufficiently long filamentation time (Rozoff *et al*., 2006) and moist convective potential, together with a sufficient low-level radial potential vorticity gradient (i.e. a beta skirt) associated with the primary swirling flow and the follow-up WISHE process. The long filamentation time and sufficient moist convective potential establish a convectively favorable environment. The beta-skirt structure and WISHE process provide a dynamical pathway to SEF. Applying the 2D turbulence theory (Huang and Robinson, 1998) to the problem of SEF in a rotating TC environment, the theme of the BSA hypothesis is that the upscale energy cascade tends to occur on the beta skirt. Following this pathway, eddy kinetic energy associated with the sporadic convective cells outside the primary eyewall may be injected into the tangential direction and enhance local low-level jets (axisymmetrized into the mean tangential flow) on the skirt of the vortex's PV profile. Once the low-level jet strengthens substantially, it can be further intensified by coupling with the boundary layer through a wind-induced moisture feedback process such as WISHE, and may ultimately lead to SEF. The time scale of this energy cascade process, and the width of the corresponding jet, can be evaluated from the values of its PV gradient. Although relevant studies have shown consistency between the evaluated and simulated jet width in Terwey and Montgomery (2008) and Qiu *et al*. (2010), direct supporting evidence for the energy upscale process described above remains to be found.

13.3.4 Unbalanced boundary layer dynamics near the top of the TC boundary layer

A deeper understanding of the boundary layer dynamics associated with SEF has been provided by two recent companion studies (WH12), based on the two mechanisms for the spin-up of azimuthal-mean tangential winds in single-eyewall TCs, highlighted in Smith *et al*. (2009). Both mechanisms are associated with the radial advection of absolute angular momentum ($M = fr^2/2 + rv$). The first mechanism applies to the spin-up above the boundary layer where M is materially conserved. The convergence of M is enhanced by the negative radial gradient of a diabatic heating rate associated with convective structures in a TC. This mechanism is the balanced dynamics (closely approximated by gradient wind and hydrostatic balance) addressed in many extant studies (cf. Section 13.3.5), and explains why the vortex expands in size. The second mechanism is related to the spin-up process within the boundary layer, and is considered to be important in the inner-core region of the storm. Although M is not materially conserved in the boundary layer, tangential winds can still be enhanced if the boundary layer inflow is sufficiently large to bring the air parcels to the small radii with minimal loss of M to friction. The boundary layer flow is coupled to the interior flow via the radial pressure gradient at the top of the boundary layer, but the spin-up of a vortex is ultimately tied to the dynamics of the boundary layer where inflow is prevailing, and the swirling wind is not in gradient wind balance over a substantial radial span.

By assimilating T-PARC (THORPEX Pacific Asian Regional Campaign; Elsberry and Harr, 2008) data (in particular, the aircraft observations) into the WRF (Weather Research and Forecasting; Skamarock *et al*., 2005) model using an ensemble Kalman filter data assimilation (as in Wu *et al*. 2010), Wu *et al*. (2012) constructed a model/observation-consistent and high-resolution spatial/temporal data set for Typhoon Sinlaku (Fig. 13.2). The following features were robustly identified in the storm's outer-core region around one day before SEF: (1) the horizontal broadening of low-level tropospheric swirling flow; and (2) intensification of boundary layer inflow over the outer region. These two important features are consistent with flow characteristics indicated in the two mechanisms, one related to balance dynamics and the other connected with unbalanced dynamics, suggested to be responsible for the spin-up of single-eyewall TCs, and to set the scene for a progressive boundary layer control pathway to SEF.

In the second of the two companion papers, Huang *et al*. (2012) addressed the association between increases in storm size and SEF from the axisymmetric viewpoint. Their findings point to collective structure changes in the outer-core region of a mature TC (Fig. 13.3), which

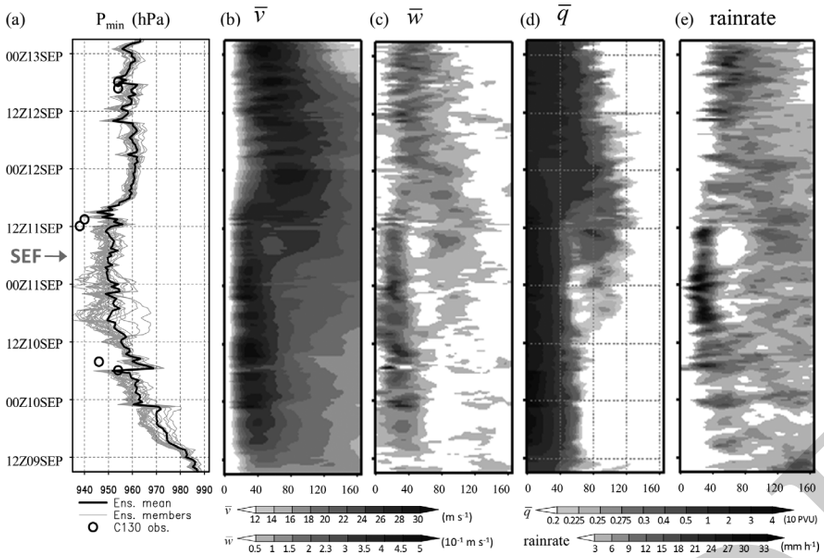

Fig. 13.2. (a) Temporal evolution of minimum sea level pressure in the control simulation of Typhoon Sinlaku (ensemble mean: black; ensemble members: gray) and C-130 flight observations (circles). Time–radius diagrams of the azimuthally mean (b) tangential wind (ms^{-1}) at the lowest model level, (c) vertical velocity (10^{-1} ms^{-1}) at a height of 0.5 km, (d) potential vorticity (10 PVU) at a height of 2 km, and (e) total column rain rate (mmh^{-1}) for the ensemble mean (average of 28 ensemble members). SEF time (0700 UTC 11 September) is indicated by an arrow on the *y*-axis (modified after Wu *et al*., 2012, their Figures 4d and 5; ©American Meteorological Society. Used with permission.)

ultimately culminates in the formation of a secondary eyewall. The sequence begins with broadening of the low-level tangential wind field associated with the intensification of the eyewall that can be demonstrated by the balanced response above the boundary layer (the first spin-up mechanism). As a result of the presence of surface friction, boundary layer inflow increases underneath the broadened swirling wind, and becomes large enough to enhance the swirling circulation within the boundary layer (the second spin-up mechanism). This rapid increase in tangential winds near the top of the boundary layer results in the local development of supergradient winds, which causes deceleration of the inflow air that is moving inward. This process leads to the transition outside the primary eyewall from sporadic and/or weak convergence in the lower troposphere to a well-defined convergence zone concentrated within, and just above, the boundary layer. This progressive increase in supergradient forces continuously provides a mechanical means for high-enthalpy air to erupt from the boundary layer. Given the dynamically and thermodynamically favorable environment for convective activity, the progressive responses of the unbalanced boundary layer flow to an expanding swirling-wind field appear to be an important mechanism for concentrating and sustaining deep convection in a narrow supergradient wind zone collocated with the SEF region. While understanding the importance of the balanced response, this study particularly noted the critical role of unbalanced dynamics in SEF. The presented progressive boundary layer control on SEF also implies that the boundary layer scheme, and its coupling to the atmosphere above, need to be adequately represented in numerical models to improve our understanding of SEF, as well as the accuracy of SEF forecasts, including the timing and preferred radial intervals.

The dynamical pathway to SEF advanced in WH12 is attractive on physical grounds, and its simplicity means that it is easy to examine. A number of recently published studies have revisited the impact of boundary layer dynamics on SEF from different perspectives. Concerning the asymmetry associated with rainbands that prevail prior to SEF, Qiu and Tan (2013) extended this SEF mechanism to include both axisymmetric and asymmetric components. The sequence of structural changes within, and just above, the boundary layer preceding SEF, and the corresponding dynamical pathway to SEF found in their simulation provided support to findings of WH12. Qiu and Tan (2013) further indicated the important role of the pre-existing outer rainbands in SEF. Wang *et al*. (2013) investigated the depth-integrated boundary layer flow, and demonstrated results that generally agree with the SEF pathway proposed in WH12. Sun *et al.* (2013) also found such an unbalanced dynamical pathway to SEF, while emphasizing how the axisymmetrization of outer rainbands and the balanced response contributed to peripheral heating in the rainbands. Forcing a slab boundary layer with a flat tangential wind profile, Abarca and Montgomery (2013) were able to generate a double-eyewall structure consistent with results from a full-physics model simulation. Taking a different point of view, Kepert (2013) indicated that the updraft in the secondary eyewall could be reasonably predicted from the gradient wind balance approximation alone. Applying a family of diagnostic boundary layer models, Kepert (2013) demonstrated that Ekman-like

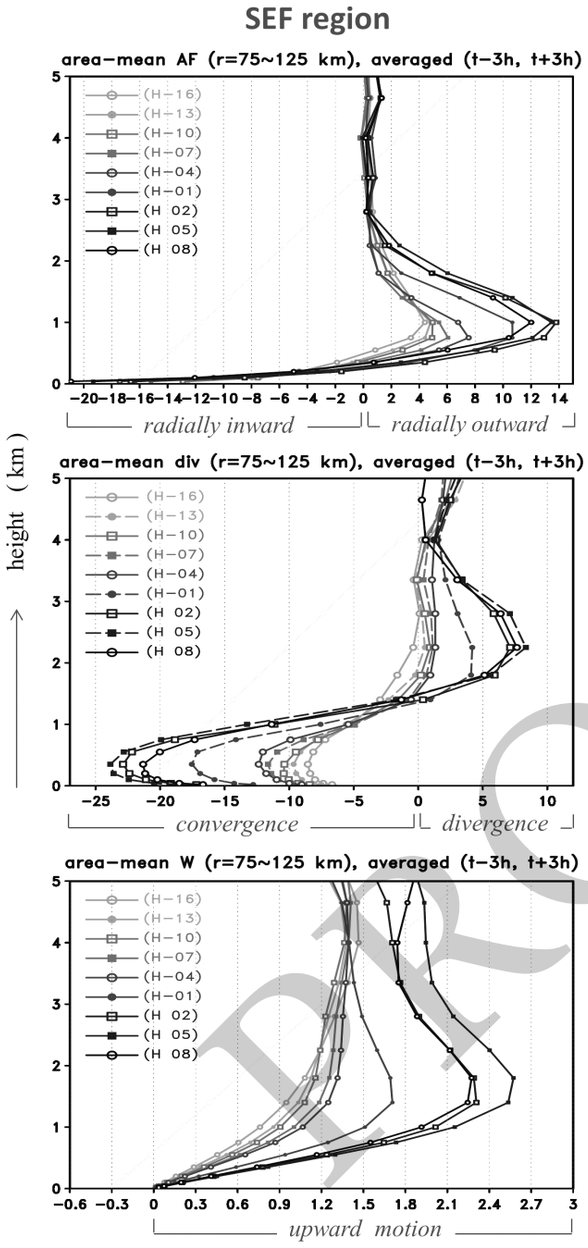

Fig. 13.3. Vertical profiles of the azimuthally, area-, and temporally averaged gradient wind (ms^{-1}; top), divergence (10^{-5} s^{-1}; middle), and vertical velocity (10^{-1} ms^{-1}; bottom) in the SEF region over (t – 3 h, t + 3 h). Results are shown from 16 h before SEF (H – 16) to 8 h after SEF (H08) (modified after Huang *et al*., 2012, their Figures 6a,c and 7a; ©American Meteorological Society. Used with permission.)

updraft in response to a small radial gradient of vorticity at the outer radii of a vortex, and the feedback between this frictionally forced updraft and the subsequent convectively generated vorticity contributes to SEF. More recently, Wu *et al*. (2014) and Kepert and Nolan (2014) re-examined the mechanism proposed by Kepert (2013) using numerical simulations with sophisticated model physical processes. Some discrepancies have been shown between these analyses. Further studies are ongoing that aim to develop a better understanding of the role of boundary layer dynamics in SEF.

13.3.5 Balanced response to diabatic heating in a region of enhanced inertial stability

Regarding balanced dynamics, the response of transverse circulation to a heating/momentum source/sink to satisfy the gradient wind and hydrostatic balance relationship (known as the Sawyer–Eliassen equation; Eliassen, 1951) has been applied to the evolution of the mean swirling circulation in idealized vortices in many previous studies (e.g. Schubert and Hack, 1982, Shapiro and Willoughby, 1982, Hack and Schubert, 1986). Rozoff *et al*. (2012) revisited the balanced dynamics of SEF from the axisymmetric viewpoint using results from cloud-resolving models. An expansion of kinetic energy (or enhanced inertial stability) had been found to occur prior to SEF in their WRF model simulation, a feature consistent with the presence of beta-skirt structure and the expansion of tangential winds mentioned in other studies. The impact of this enhanced kinetic energy and diabatic heating on SEF was further investigated with a symmetric linearized nonhydrostatic model (a balanced vortex model similar to the Sawyer–Eliassen model). Given the axisymmetric tangential wind and temperature profiles from the WRF model output, this simple model depicts how the transverse circulation responds to diabatic heating and surface friction, which are forcings prescribed by the WRF simulation. The diagnosed results are similar to the mean vortex structure in the WRF simulation in a number of ways, and suggest that the sustained diabatic heating, along with the broadening wind outside the primary eyewall, contribute most to the enhancement of tangential winds in the SEF region. Conducting the same analysis, Sun *et al*. (2013) demonstrated supporting results based on a WRF simulation of Typhoon Sinlaku.

13.4 Concluding remarks

In addition to the above discussion, other perspectives exist that are not categorized as environmental conditions or internal dynamics for SEF, but are still worth noting. Houze *et al*. (2007) indicated that their model simulation failed to capture the eyewall replacement cycle of Hurricane Rita (2005) when the horizontal resolution was reduced from 1.67 to 5 km. Meanwhile, it was speculated that the small-scale features shown in the radar data during

Rita's eyewall replacement cycle may be related to the VRW dynamics. The importance of increasing model resolution, and the value of targeting small-scale structures in TCs, are suggested as likely factors in the future improvement of our understanding of SEF and the subsequent eyewall replacement cycle. Details of the microphysical processes used in the models have shown that they affect the timing and locations of SEF, the intensity of eyewalls, and the duration of an eyewall replacement cycle (Willoughby *et al*., 1984, Terwey and Montgomery, 2008, Zhou and Wang, 2011, Fang and Zhang, 2012).

The environmental conditions and internal mechanisms suggested as being responsible for SEF in existing studies are briefly summarized below. Regarding the environmental control of SEF, model initial relative humidity has been shown to be critical to the increase of storm size and the subsequent SEF in recent studies using sophisticated numerical models. In contrast, a variety of different approaches have been proposed as the internal mechanisms of SEF, including: (1) axisymmetrization of prescribed/present outer vorticity patches; (2) the accumulation of eddy kinetic energy associated with VRWs near their stagnation radii; (3) the energy cascade process over the beta skirt of the TC vortex in a convectively favorable condition and subsequent positive feedback provided by WISHE (BSA hypothesis); (4) the unbalanced response (i.e. the generation of supergradient wind, and its impact on the transverse circulation) to the expanding winds; and (5) the balanced response of transverse circulation to diabatic heating over the area with enhanced inertial stability. Particularly noteworthy is that the broadening tangential wind (the beta-skirt structure and enhanced kinetic energy basically indicate a similar structure as well) furnishing the pathway to SEF is a consistently vital process among the various internal dynamical interpretations of SEF. Several conditions and mechanisms have been suggested for the establishment of such a skirted vortex structure, including higher environmental relative humidity or diabatic heating associated with outer rainbands, the initial vortex size/shape, concurrent storm intensity, convective heating in an intensifying storm, and radially outward-propagating VRWs.

Although recent advances in the unbalanced and balanced dynamics of TCs with double eyewalls appear promising for the interpretation of SEF from the axisymmetric perspective, the quantitative impacts of these factors on SEF and their mutual feedback require further investigation. While axisymmetric dynamics have been shown to play a critical role in SEF, the question of how the asymmetric components (e.g. spiral rainbands and sporadic convective cells in the vortex's outer-core region) influence SEF also requires further study if we are to develop a more comprehensive understanding of SEF. While the environmental conditions are relatively well understood and better presented in the observations and numerical models, discoveries are also being made of more uncertainties associated with the evolution of a TC vortex and the accompanying convective-scale features. More TC observations and further investigation of internal vortex dynamics are required if we are to better present the corresponding physical processes (e.g. microphysics, boundary layer dynamics) in numerical simulations of SEF, as well as the whole TC life-cycle.

13.5 Acknowledgment

Chun-Chieh and Yi-Hsuan were supported by the National Science Council of Taiwan under Grant NSC102-2628-M-002-008.

References

Abarca, S. F. and Corbosiero, K. L. (2011). Secondary eyewall formation in WRF simulations of hurricanes Rita and Katrina (2005). *Geophys. Res. Lett.*, **38**, L07802, doi:10.1029/2011GL047015.

Abarca, S. F. and Montgomery, M. T. (2013). Essential dynamics of secondary eyewall formation. *J. Atmos. Sci.*, **70**, 3216–3230.

Black, M. L. and Willoughby, H. E. (1992). The concentric eyewall cycle of Hurricane Gilbert. *Mon. Wea. Rev.* **120**, 947–957.

Bell, M. M., Montgomery, M. T., and Lee, W.-C. (2012). An axisymmetric view of eyewall evolution in Hurricane Rita (2005). *J. Atmos. Sci.*, **8**, 2414–2432.

Chen, Y. and Yau, M. K. (2001). Spiral bands in a simulated hurricane. Part I: Vortex Rossby wave verification, *J. Atmos. Sci.*, **58**, 2128–2145.

Chen, Y., Brunet, G., and Yau, M. K. (2003). Spiral bands in a simulated hurricane. Part II: Wave activity diagnostics, *J. Atmos. Sci.*, **60**, 1239–1256.

Corbosiero, K. L., Molinari, J., Aiyyer, A. R., and Black, M. L. (2006). The structure and evolution of Hurricane Elena (1985). Part II: Convective asymmetries and evidence for vortex Rossby waves. *Mon. Wea. Rev.*, **134**, 3073–3091.

Corbosiero, K. L., Abarca, S., and Montgomery, M. T. (2012). Vortex Rossby waves and secondary eyewall formation in a high-resolution simulation of Hurricane Katrina (2005). 30th Conference on Hurricanes and Tropical Meteorology. Amer. Meteor. Sco., Jacksonville, FL. 1A.6.

Didlake, A. C. and Houze, R. A., Jr. (2011). Kinematics of the secondary eyewall observed in Hurricane Rita (2005). *J. Atmos. Sci.*, **68**, 1620–1636.

Dritschel, D. G. and Waugh, D. (1992). Quantification of the inelastic interaction of unequal vortices in two-dimensional vortex dynamics. *Phys. Fluids*, **4A**, 1737–1744.

Eliassen, A. (1951). Slow thermally or frictionally controlled meridional circulation in a circular vortex. *Astrophys. Norv.*, **5**, 19–60.

Elsberry R. L. and Harr, P. A. (2008). Tropical cyclone structure (TCS08) field experiment science basis, observational platforms, and strategy. Asia-Pacific *J. Atmos. Sci.*, **44**, 3, 209–231.

Fang, J. and Zhang, F. (2012). Effect of beta shear on simulated tropical cyclones. *Mon. Wea. Rev.*, **140**, 3327–3346.

Fuentes, O. U. V. (2004). Vortex filamentation its onset and its role on axisymmetrization and merger. *Dyn. Atmos. Oceans*, **40**, 23–42.

Hack, J. J. and Schubert, W. H. (1986). Nonlinear response of atmospheric vortices to heating by organized cumulus convection. *J. Atmos. Sci.*, **43**, 1559–1573.

Hawkins, J. D. and Helveston, M. (2008). Tropical cyclone multiple eyewall characteristics. 28th Conf. on Hurricanes and Tropical Meteorology, Orlando, FL. *Amer. Meteor. Soc.*, 14B.1.

Hence, D. A. and Houze, R. A., Jr. (2012). Vertical structure of tropical cyclones with concentric eyewalls as seen by the TRMM precipitation radar. *J. Atmos. Sci.*, **69**, 1021–1036.

Hill, K. A. and Lackmann, G. M. (2009). Influence of environmental humidity on tropical cyclone size. *Mon. Wea. Rev.*, **137**, 3294–3315.

Houze, R. A., Jr., Chen, S. S., Lee, W.-C., *et al*. (2006). The Hurricane Rainband and Intensity Change Experiment: Observations and modeling of Hurricanes Katrina, Ophelia, and Rita. *Bull. Am. Meteor. Soc.* **87**, 1503–1521.

Houze, R. A., Jr., Chen, S. S., Smull, B. F., Lee, W.-C., and Bell, M. M. (2007). Hurricane intensity and eyewall replacement, *Science*, **315**, 1235–1239.

Huang, H.-P. and Robinson, W. A. (1998). Two-dimensional turbulence and persistent zonal jets in a global barotropic model, *J. Atmos. Sci.*, **55**, 611–632.

Huang, Y.-H., Montgomery, M. T., and Wu, C.-C. (2012). Concentric eyewall formation in Typhoon Sinlaku (2008). Part II: Axisymmetric dynamical processes. *J. Atmos. Sci.*, **69**, 662–674.

Kepert, J. D. (2013). How does the boundary layer contribute to eyewall replacement cycles in axisymmetric tropical cyclones? *J. Atmos. Sci.*, **70**, 2808–2830.

Kepert, J. D. and Nolan, D. S. (2014). Analysis of a simulated tropical cyclone eyewall replacement cycle. 31st Conference on Hurricanes and Tropical Meteorology. Amer. Meteor. Sco., San Diego, CA. 11C.3.

Kossin, J. P. and Sitkowski, M. (2009). An objective model for identifying secondary eyewall formation in hurricanes. *Mon. Weather Rev.*, **137**, 876–892.

Kuo, H.-C., Lin, L.-Y., Chang, C.-P., and Williams, R. T. (2004). The formation of concentric vorticity structures in typhoons. *J. Atmos. Sci.*, **61**, 2722–2734.

Kuo, H.-C., Schubert, W. H., Tsai, C.-L., and Kuo, Y.-F. (2008). Vortex interaction and barotropic aspects of concentric eyewall formation. *Weather Rev.,* **137**, 5182–5198.

Kuo, H.-C., Chang, C.-P., Yang, Y.-T. and Jiang, H.-J. (2009). Western North Pacific typhoons with concentric Eyewalls. *Mon. Weather Rev.*, **137**, 3758-3770.

Judt, F. and Chen, S. S. (2010). Convectively generated potential vorticity in rainbands and formation of the secondary eyewall in Hurricane Katrina of 2005. *J. Atmos. Sci.*, **67**, 3581–3599.

MacDonald, N. J. (1968). The evidence for the existence of Rossby type waves in the hurricane vortex. *Tellus*, **20**, 138–150.

Martinez, Y., Brunet, G., and Yau, M. K. (2010). On the dynamics of two-dimensional hurricane-like concentric rings vortex formation. *J. Atmos. Sci.*, **67**, 3253–3268.

Martinez, Y., Brunet, G., Yau, M. K., and Wang, X. (2011). On the dynamics of concentric eyewall genesis: Space-time empirical normal modes diagnosis. *J. Atmos. Sci.*, **68**, 457–476.

McWilliams, J. C. (1990). The vortices of two-dimensional turbulence. *J. Fluid. Mech.*, **219**, 361–385.

Melander, M. V., McWilliams, J. C., and Zabusky, N. J. (1987). Axisymmetrization and vorticity-gradient intensification of an isolated two-dimensional vortex through filamentation. *J. Fluid Mech.*, **178**, 137–159.

Menelaou, K., Yau, M. K., and Martinez, Y. (2012). On the dynamics of the secondary eyewall genesis in Hurricane Wilma (2005). *Geophys. Res. Lett.*, **39**, L04801, doi:10.1029/2011GL050699.

Menelaou, K., Yau, M. K., and Martinez, Y. (2013). Impacts of asymmetric dynamical processes on the structure and intensity change of two-dimensional hurricane-like annular vortices. *J. Atmos. Sci.*, **70**, 559–582.

Montgomery, M. T. and Kallenbach, R. J. (1997). A theory for vortex Rossby waves and its application to spiral bands and intensity changes in hurricanes, *Q. J. R. Meteorol. Soc.,* **123**, 435– 465.

Moon, Y., Nolan, D. S., and Iskandarani, M. (2010). On the use of two-dimensional incompressible flow to study secondary eyewall formation in tropical cyclones. *J. Atmos. Sci.*, **67**, 3765–3773.

Nong, S. and Emanuel, K. A. (2003). A numerical study of the genesis of concentric eyewalls in hurricane. *Quart. J. Roy. Meteor. Soc.*, **129**, 3323–3338.

Qiu, X., Tan, Z.-M., and Xiao, Q. (2010). The roles of vortex Rossby waves in Hurricane secondary eyewall formation. *Mon. Wea. Rev.*, **138**, 2092–2019.

Qiu, X. and Tan, Z.-M. (2013). The roles of asymmetric inflow forcing induced by outer rainbands in tropical cyclone secondary eyewall formation. *J. Atmos. Sci.*, **70**, 953–974.

Rozoff, C. M., Schubert, W. H., McNoldy, B. D., and Kossin, J. P. (2006). Rapid filamentation zones in intense tropical cyclones. *J. Atmos. Sci.*, **63**, 325–340.

Rozoff, C. M., Nolan, D. S., Kossin, J. P., Zhang, F., and Fang, J. (2012). The roles of an expanding wind field and inertial stability in tropical cyclone secondary eyewall formation. *J. Atmos. Sci.*, **69**, 2621–2643.

Schubert, W. H. and Hack, J. J. (1982). Inertial stability and tropical cyclone development. *J. Atmos. Sci.*, **39**, 1687–1697.

Shapiro, L. J. and Willoughby, H. E. (1982). The response of balanced hurricanes to local sources of heat and momentum. *J. Atmos. Sci.*, **39**, 378–394.

Sikowstki, M., Kossin, J. P., and Rozoff, C. M. (2011). Intensity and structure changes during hurricane eyewall replacement cycles. *Mon. Wea. Rev.*, **139**, 3829–3847.

Skamarock, W. C., Klemp, J. B., Dudhia, J., *et al*. (2005). A description of the Advanced Research WRF Version 2. NCAR Tech. NoteNCAR/TN-4681ST, 88 pp.

Smith, R. K., Montgomery, M. T., and Nguyen, S. V. (2009). Tropical cyclone spin-up revisited. *Q. J. R. Meteorol. Soc.* **135**, 1321–1335.

Sun, Y. Q., Jiang, Y., Tan, B., and Zhang, F. (2013). The governing dynamics of the secondary eyewall formation of Typhoon Sinlaku (2008). *J. Atmos. Sci.*, **70**, 3818–3837.

Terwey, W. D. and Montgomery, M. T. (2008). Secondary eyewall formation in two idealized, full-physics modeled hurricanes. *J. Geophys. Res.*, **113**, D12112.

Wang, Y. (2002a). Vortex Rossby waves in a numerically simulated tropical cyclone. Part I: Overall structure, potential vorticity, and kinetic energy budgets. *J. Atmos. Sci.*, **59**, 1213–1238.

Wang, Y. (2002b). Vortex Rossby waves in a numerically simulated tropical cyclone. Part II: The role in tropical cyclone structure and intensity changes. *J. Atmos. Sci.*, **59**, 1239–1262.

Wang, Y. (2009). How do outer spiral rainbands affect tropical cyclone structure and intensity? *J. Atmos. Sci.*, **66**, 1250–1273.

Wang, X., Ma, Y., and Davidson, N. E. (2013). Secondary eyewall formation and eyewall replacement cycles in a simulated hurricane: effect of the net radial force in the hurricane boundary layer. *J. Atmos. Sci.* (http://dx.doi.org/10.1175/JAS-D-12-017.1) (in press)

Willoughby, H. E., Clos, J. A., and Shoreibah, M. G. (1982). Concentric eyewalls, secondary wind maxima, and the evolution of the hurricane vortex, *J. Atmos. Sci.,* **39**, 395–411.

Willoughby, H. E., Jin, H.-L., Lord, S. J., and Piotrowicz, J. M. (1984). Hurricane structure and evolution as simulated by an axisymmetric, nonhydrostatic numerical model, *J. Atmos. Sci.,* **41**, 1169–1186.

Willoughby, H. E. and Black, P. G. (1996). Hurricane Andrew in Florida: Dynamics of a disaster, *Bull. Am. Meteorol. Soc.,* **77**, 543–549.

Wu, C.-C., Cheng, H.-J., Wang, Y., and Chou, K.-H. (2009). A numerical investigation of the eyewall evolution in a landfalling typhoon. *Mon. Wea. Rev.*, **137**, 21–40.

Wu, C.-C., Lien, G.-Y., Chen, J.-H., and Zhang, F. (2010). Assimilation of tropical cyclone track and structure based on the Ensemble Kalman Filter (EnKF). *J. Atmos. Sci.,* **67**, 3806–3822.

Wu, C.-C., Huang, Y.-H., and Lien, G.-Y. (2012). Concentric eyewall formation in Typhoon Sinlaku (2008). Part I: Assimilation of T-PARC data based on the ensemble Kalman filter (EnKF). *Mon. Wea. Rev.,* **140**, 506–527.

Wu, C.-C., Kuan, S.-P., Cheng, Y.-M., and Huang, Y.-H. (2014). Unbalanced dynamics of secondary eyewall formation in tropical cyclones- Part II: Analyses from higher-resolution simulations. 31st Conference on Hurricanes and Tropical Meteorology. Amer. Meteor. Sco., San Diego, CA. 11C.2.

Yano, J.-I. and Emanuel, K. A. (1991). An improved model of the equatorial troposphere and its coupling with the stratosphere, *J. Atmos. Sci.,* **48**, 377– 389.

Zhou, X. and Wang, B. (2011). Mechanism of concentric eyewall replacement cycles and associated intensity change. *J. Atmos. Sci.*, **68**, 972–988.